

THE DIFFUSE GAMMA-RAY FLUX ASSOCIATED WITH SUB-PEV/PEV NEUTRINOS FROM STARBURST GALAXIES

XIAO-CHUAN CHANG^{1,2}, XIANG-YU WANG^{1,2}

¹ School of Astronomy and Space Science, Nanjing University, Nanjing, 210093, China; xywang@nju.edu.cn

² Key laboratory of Modern Astronomy and Astrophysics (Nanjing University), Ministry of Education, Nanjing 210093, China

Draft version December 3, 2024

ABSTRACT

One attractive scenario for the excess of sub-PeV/PeV neutrinos recently reported by IceCube is that they are produced by cosmic rays in starburst galaxies colliding with the dense interstellar medium. This proton-proton (pp) collision also produces high-energy gamma-rays, which finally contribute to the diffuse high-energy gamma-ray background. It was shown that they contribute $\gtrsim 40\%$ of the observed diffuse gamma-ray background in the 100 GeV range observed by Fermi/LAT. We re-calculate the diffuse gamma-ray flux by considering that the very high energy gamma-rays will be absorbed in the galaxies and converted into electron-positron pairs, which then lose almost all their energy through synchrotron radiation in the strong magnetic fields in the starburst region. Since the synchrotron emission goes into energies below GeV, this synchrotron loss reduce the diffuse high-energy gamma-ray flux. For a E_ν^{-2} neutrino spectrum, we find that the diffuse gamma-ray flux contribute about 20% of the observed diffuse gamma-ray background in the 100 GeV range, thus leaving more room for other sources to contribute to the gamma-ray background. However, for a steeper neutrino spectrum, this synchrotron loss effect is less important, since the energy fraction in absorbed gamma-rays becomes lower.

Subject headings: neutrinos- cosmic rays

1. INTRODUCTION

The IceCube Collaboration reported 37 events ranging from 60 TeV to 3 PeV within three years of operation, correspond to a 5.7σ excess over the background atmospheric neutrinos and muons (Aartsen et al. 2014). The observed events can be fitted by a hard spectra ($E_\nu^{-\Gamma}$) with $\Gamma = 2$ and a cutoff above 2 PeV, implied by the non-detection of higher energy events, or alternatively by a slightly softer but unbroken power-law spectrum with index $\Gamma \simeq 2.2 - 2.3$ (Aartsen et al. 2014; Anchordoqui et al. 2014a). The best-fit single-flavor astrophysical flux ($\nu + \bar{\nu}$) is $E_\nu^2 \Phi_\nu = 0.95 \pm 0.3 \times 10^{-8} \text{GeVcm}^{-2} \text{s}^{-1} \text{sr}^{-1}$, assuming a E_ν^{-2} spectrum. The sky distribution of the these events is consistent with isotropy (Aartsen et al. 2014), implying an extragalactic origin or possibly Galactic halo origin (Taylor et al. 2014), although a fraction of them could come from Galactic sources (Fox et al. 2013; Ahlers & Murase 2013; Neronov et al. 2014; Razzaque 2013; Lunardini et al. 2013). The source of these IceCube neutrinos is, however, unknown. Jets and/or cores of active galactic nuclei (AGN), and gamma-ray burst (GRBs) have been suggested to be possible sources (Stecker et al. 1991; Anchordoqui et al. 2008; Kalashev et al. 2013; Stecker 2013; Waxman & Bahcall 1997; He et al. 2012; Murase & Ioka 2013; Liu & Wang 2013), where the photo-hadronic (e.g., $p\gamma$) reaction is typically the main neutrino generation process (Winter 2013). On the other hand, starburst galaxies and galaxy clusters may also produce PeV neutrinos, mainly via the hadronuclear (e.g., pp) reaction (He et al. 2013; Murase et al. 2013; Liu et al. 2014; Tamborra et al. 2014; Anchordoqui et al. 2014b). In this paper, we concern the pp process in starburst galaxies, following earlier works in which supernovae in general (Loeb & Waxman 2006) or a special class of supernova-hypernovae (Liu et al. 2014) in starburst galaxies accelerate

cosmic rays (CRs), which in turn produce neutrinos by interacting with the dense surrounding medium during propagation in their host galaxies. To produce PeV neutrinos, we require a source located at redshift z to accelerate protons to energies of $50(1+z)/2$ PeV. It is suggested that semi-relativistic hypernova remnants in starburst galaxies, by virtue of their fast ejecta, can accelerate protons to EeV energies (Wang et al. 2007; Liu & Wang 2012). Alternatively, assuming sufficient amplification of the magnetic fields in the starburst region, normal supernova remnants may also be able to accelerate protons to 10^{17} eV and produce PeV neutrinos (Murase et al. 2013).

In pp collisions, charged and neutral pions are both generated. Charged pions decay to neutrinos ($\pi^+ \rightarrow \nu_\mu \bar{\nu}_\mu \nu_e e^+$, $\pi^- \rightarrow \bar{\nu}_\mu \nu_\mu \bar{\nu}_e e^-$), while neutral pions decay to gamma-rays ($\pi^0 \rightarrow \gamma\gamma$). Thus, PeV neutrinos are accompanied by high-energy gamma-rays. For a E_ν^{-2} neutrino spectrum with a single-flavor flux of $E_\nu^2 \Phi_\nu \simeq 10^{-8} \text{GeVcm}^{-2} \text{s}^{-1} \text{sr}^{-1}$ produced by π^\pm decay, the flux of gamma-rays from π^0 -decay is $2 \times 10^{-8} \text{GeVcm}^{-2} \text{s}^{-1} \text{sr}^{-1}$. While low-energy gamma-rays may escape freely from the galaxy, the very high energy (VHE) gamma-rays will be absorbed by the soft photons in starbursts. The absorbed gamma-rays will convert to electron-positron (e^\pm) pairs, which then initiate electromagnetic cascades on soft background photons, reprocessing the energy of high-energy photons to observable diffuse gamma rays. Since the cascade gamma-ray spectrum is nearly flat (i.e., $\Phi_\gamma \propto E_\gamma^{-\alpha_\gamma}$ with $\alpha_\gamma \sim 1.8 - 2$) (Berezinskii & Smirnov 1975; Coppi & Aharonian 1997), the additional contribution to the gamma-ray background flux by the cascade emission is also roughly $2 \times 10^{-8} \text{GeVcm}^{-2} \text{s}^{-1} \text{sr}^{-1}$. Another component that can contribute to the diffuse gamma-ray emission is e^\pm pairs produced simultaneously with the neutrinos in the π^\pm decay. The IC scatterings of these pairs with infrared

photons will produce very high energy photons, which may be absorbed and finally contribute to the cascade gamma-ray component with a flux $\sim 10^{-8}\text{GeVcm}^{-2}\text{s}^{-1}\text{sr}^{-1}$. Noting that the observed gamma-ray background flux by Fermi/LAT is $\sim 10^{-7}\text{GeVcm}^{-2}\text{s}^{-1}\text{sr}^{-1}$ at $\sim 100\text{ GeV}$ (Abdo et al. 2010), the total diffuse gamma-ray flux associated with PeV neutrinos in the pp scenario would thus contribute $\sim 50\%$ of the observed diffuse gamma-ray background in the $\sim 100\text{ GeV}$ range, which is consistent with the results in Murase et al. (2013) and Liu et al. (2014). Since other sources, such as AGNs (Stecker & Salamon 1996) or truly diffuse gamma-ray emission from the propagation of ultra-high energy cosmic rays (UHECRs) in cosmic microwave and infrared background radiation (Berezinskii & Smirnov 1975; Kalashev et al. 2009; Berezhinsky et al. 2011; Wang et al. 2011), also contribute significantly to the diffuse gamma-ray background, a tension between a too high diffuse gamma-ray flux expected from sources and the observed background flux exists.

In this paper, we calculate the accumulative diffuse gamma-ray flux by considering the synchrotron loss of e^\pm produced by the absorbed gamma-rays in the magnetic fields of the starburst region. For reasonable assumptions of the strength of the magnetic fields in the starburst region, we find that the synchrotron loss dominates over the inverse-Compton (IC) scattering loss. Since the synchrotron emission goes into energies below GeV, the intensity of the cascade gamma-ray component is significantly reduced in the $\sim 100\text{ GeV}$ energy range. In §2, we first obtain the normalization of the gamma-ray flux of an individual starburst galaxy with the observed neutrino flux. In §3, we calculate the gamma-ray flux after considering the synchrotron loss. Then in §4, we calculate the accumulative gamma-ray flux from the population of starburst galaxies. Finally we give our conclusions and discussions in §5.

2. NORMALIZATION

To calculate the accumulative diffuse gamma-ray flux, we need to know the the gamma-ray flux from individual starburst galaxies and then integrate over contributions by all the starburst galaxies in the Universe. The gamma-ray flux of an individual galaxy can be then calibrated with the observed neutrino flux, assuming that all the observed neutrinos by IceCube are produced by starburst galaxies.

As the neutrino flux is linearly proportionally to the cosmic-proton flux and the efficiency in transferring the proton energy to secondary pions, the single-flavor neutrino ($\nu + \bar{\nu}$) flux from a starburst galaxy is expressed by

$$\Phi_{\nu_i} = \frac{dN_{\nu_i}}{dt dE_\nu} \propto f_\pi L_p E_\nu^{-p}, \quad (1)$$

where $i = (e, \mu, \tau)$, L_p is the CR proton flux at some fixed energy and f_π is the pion production efficiency. p is the index of the proton spectrum ($dn/dE_p \propto E_p^{-p}$), and we assume $p = 2$, as expected from Fermi acceleration, unless otherwise specified. Starbursts have very high star formation rates (SFR) of massive stars. Massive stars produce supernova or hypernovae, which accelerate CRs in the remnant blast waves, so we expect that $L_p \propto SFR$. On the other hand, the radiation of a large population of hot young stars are absorbed by dense dust and reradiated in the infrared band, so $L_{\text{TIR}} \propto SFR$, where L_{TIR} is the total infrared luminosity of the starburst galaxy. Thus we expect that $L_p \propto L_{\text{TIR}}$, so

$$\Phi_{\nu_i}(E_\nu, L_{\text{TIR}}) = C_1 f_\pi \frac{L_{\text{TIR}}}{L_\odot} \left(\frac{E_\nu}{1\text{GeV}} \right)^{-p}, \quad (2)$$

where C_1 is the normalization factor and L_\odot is the bolometric luminosity of the Sun. The photopion efficiency is $f_\pi = 1 - \exp(-t_{\text{esc}}/t_{\text{loss}})$, where t_{loss} is the energy-loss time for pp collisions and t_{esc} is the escape time of protons. $t_{\text{loss}} = (0.5 n \sigma_{pp} c)^{-1}$, where the factor 0.5 is inelasticity, n is the particle density of gas and σ_{pp} is the inelastic proton collision cross section, which is insensitive to proton energy. Introducing a parameter $\Sigma_g = m_p n R$ as the surface mass density of the gas (where R is the length scale of the starburst region), the energy loss time is

$$t_{\text{loss}} = 7 \times 10^4 \text{yr} \frac{R}{500 \text{pc}} \left(\frac{\Sigma_g}{1 \text{gcm}^{-2}} \right)^{-1}. \quad (3)$$

We use $R = 500\text{pc}$ as the reference value¹ because neutrinos are dominantly produced by high redshift starbursts, as implied by the star-formation history, and high redshift starburst typically have $R \sim 500\text{pc}$ (Tacconi et al. 2006). There are two ways for CRs to escape from a galaxy. One is the advective escape via a galactic wind and the other is the diffusive escape. The advective escape time is

$$t_{\text{adv}} = R/v_w = 4.5 \times 10^5 \text{yr} \frac{R}{500 \text{pc}} \left(\frac{v_w}{1000 \text{kms}^{-1}} \right)^{-1}, \quad (4)$$

where v_w is the velocity of galactic wind. One can see that protons lose almost all their energy in dense starburst galaxies with $\Sigma_g \gtrsim 0.15(v_w/1000\text{kms}^{-1})\text{gcm}^{-2}$, if the advective time is shorter than the diffusive escape time. Little is known about the diffusive escape time in starbursts. The diffusive escape time can be estimated as $t_{\text{diff}} = R^2/2D$, where $D = D_0(E/E_0)^\delta$ is the diffusion coefficient, D_0 and E_0 are normalization factors, and $\delta = 0-1$ depending on the spectrum of interstellar magnetic turbulence. As in Liu et al. (2014) and Murase et al. (2013), we assume a lower diffusion coefficient $D_0 \lesssim 10^{27}\text{cm}^2\text{s}^{-1}$ at $E_0 = 3\text{GeV}$ for high redshift starburst galaxies, because the magnetic fields in nearby starburst galaxies such as M82 and NGC253 are observed to be 100 times stronger than in our Galaxy, and the diffusion coefficient is expected to scale with the CR Larmor radius ($\propto E_p/B$). The diffusive escape time is thus

$$t_{\text{diff}} = 10^5 \text{yr} \left(\frac{R}{500 \text{pc}} \right)^2 \left(\frac{D_0}{10^{27}\text{cm}^2\text{s}^{-1}} \right)^{-1} \left(\frac{E_p}{60\text{PeV}} \right)^{-0.3} \quad (5)$$

for $\delta = 0.3$ (Trotta et al. 2011). Alternatively, Lacki et al. (2011) assume that CRs stream out the starbursts at the average Alfvén speed $v_A = B/\sqrt{4\pi m_p n}$, so

$$t_{\text{diff}} = 2.2 \text{Myr} \left(\frac{R}{500 \text{pc}} \right)^{1/2} \left(\frac{\Sigma_g}{1 \text{gcm}^{-2}} \right)^{1/2} \left(\frac{B}{2 \text{mG}} \right)^{-1}, \quad (6)$$

where B is the magnetic field in the starburst region. The escape time is the minimum of the advective time and the diffusive time, i.e. $t_{\text{esc}} = \min(t_{\text{adv}}, t_{\text{diff}})$.

The accumulative neutrino flux can be estimated by summing up the contribution by all starburst galaxies throughout the whole universe, i.e.

$$E_\nu^2 \Phi_{\nu_i}^{\text{accu}} = \frac{E_\nu^2 c}{4\pi} \int_0^{z_{\text{max}}} \int_{L_{\text{TIR}, \text{min}}}^{L_{\text{TIR}, \text{max}}} \frac{\phi(L_{\text{TIR}}, z) \Phi_{\nu_i} [(1+z)E_\nu, L_{\text{TIR}}]}{H_0 \sqrt{(1+z)^3 \Omega_M + \Omega_\Lambda}} dL_{\text{TIR}} dz, \quad (7)$$

¹ For comparison, we also consider $R = 200\text{pc}$ in the following calculations.

where $\phi(L_{\text{TIR}}, z)$ represents the luminosity function of starburst, $H_0 = 71 \text{ km s}^{-1} \text{ Mpc}^{-1}$, $\Omega_M = 0.27$, $\Omega_\Lambda = 0.73$. Herchel PEP/HerMES has recently provided an estimation of the IR-galaxy luminosity function for separate classes (Gruppioni et al. 2013), which is a modified-Schechter function

$$\phi(L_{\text{TIR}}) = \phi^* \left(\frac{L_{\text{TIR}}}{L^*} \right)^{1-\alpha} \exp \left[-\frac{1}{2\sigma^2} \log_{10}^2 \left(1 + \frac{L_{\text{TIR}}}{L^*} \right) \right]. \quad (8)$$

For starburst galaxies, $\alpha = 1.00 \pm 0.20$, $\sigma = 0.35 \pm 0.10$, $\log_{10}(L^*/L_\odot) = 11.17 \pm 0.16$, $\log_{10}(\phi^*/\text{Mpc}^{-3} \text{ dex}^{-1}) = -4.46 \pm 0.06$. L^* evolves with redshift as $\propto (1+z)^{k_L}$ with $k_L = 1.96 \pm 0.13$. For ϕ^* , it evolves as $\propto (1+z)^{k_{\rho,1}}$ when $z < z_{b,\rho}$, and as $\propto (1+z)^{k_{\rho,2}}$ when $z > z_{b,\rho}$, with $k_{\rho,1} = 3.79 \pm 0.21$, $k_{\rho,2} = -1.06 \pm 0.05$ and $z_{b,\rho} = 1$. We set $z_{\text{max}} = 4$ and the luminosity ranges from $10^{10} L_\odot$ to $10^{14} L_\odot$.

We assume all the observed neutrinos are produced by starburst galaxies, so we can normalize the accumulative diffuse neutrino flux in Eq. (7) with the observed flux at PeV energy, i.e.

$$E_\nu^2 \Phi_{\nu_i} |_{E_\nu=1 \text{ PeV}} = 0.95 \times 10^{-8} \text{ GeV cm}^{-2} \text{ s}^{-1} \text{ sr}^{-1}. \quad (9)$$

Using the central values of the above parameters in the luminosity function (e.g. $\alpha = 1.00$, $\sigma = 0.35$ and $\log_{10}(L^*/L_\odot) = 11.17$), we get $C_1 = 4.1 \times 10^{21} \text{ eV}^{-1} \text{ s}^{-1}$ for $p = 2$. Varying the values of these parameters within their error, the value of C_1 changes within a factor of a few. However, we note that the result of the accumulative gamma-ray flux, as calculated below in §4, remains almost unchanged. We also find that the spectrum of the accumulative neutrino flux, as given by Eq.(7), is flat ($\propto E_\nu^{-2}$) for either choice of the diffusive escape times in Eq.(5) or Eq.(6).

For pp collisions, the energy flux in π^0 -decay gamma-rays is $E_\gamma^2 \Phi_\gamma \propto (1/3) E_p Q_p$, where Q_p represents the differential CR energy flux. Since the neutrino flux is $E_\nu^2 \Phi_\nu \propto (1/6) E_p Q_p$, the gamma-ray flux resulted from the π^0 -decay is related to the neutrino flux by

$$E_\gamma^2 \Phi_\gamma \approx 2 E_\nu^2 \Phi_{\nu_i} |_{E_\nu=0.5 E_\gamma}. \quad (10)$$

Thus the π^0 -decay gamma-ray flux of a single starburst should be

$$\Phi_\gamma = 8.2 \times 10^{21} f_\pi \frac{L_{\text{TIR}}}{L_\odot} \left(\frac{E_\gamma}{1 \text{ GeV}} \right)^{-2} \quad (11)$$

for $p = 2$.

3. GAMMA-RAY FLUX FROM ONE SINGLE STARBURST GALAXY

The pp process produces neutral pions π^0 and charged pions π^\pm . The neutral pion decay produces gamma-rays. Besides, e^\pm pairs from the decay of π^\pm , can also produce gamma-rays through IC scattering off the soft photons in the starburst region, mainly the infrared photons (in competing with the synchrotron radiation in the magnetic field). While the low-energy gamma-rays can escape and contribute to the diffuse gamma-ray background, the VHE gamma-rays will be absorbed due to the dense photon field in the starburst region. The absorbed gamma-rays will be converted into e^\pm pairs, which initiate cascades through interactions with the soft photons. As the VHE gamma-rays cascade down to enough low energies, they can escape out of the starburst and also contribute to the diffuse gamma-ray background. Below we con-

sider the separate contributions by the absorbed gamma-rays and the unabsorbed ones.

3.1. Absorption of high-energy gamma-rays in starbursts

Rapid star formation process makes an intense infrared photon field in the starburst. The VHE gamma-ray photons may be absorbed by background photons and generate e^\pm pairs. The optical depth is $\tau_{\gamma\gamma}(E_\gamma) = \int \sigma_{\gamma\gamma}(\varepsilon, E_\gamma) n(\varepsilon) R d\varepsilon$, where $\sigma_{\gamma\gamma}$ is the cross section for pair-production (Bonometto & Rees 1971; Schlickeiser et al. 2012) and $n(\varepsilon)$ is the number density the infrared background photons. We adopt the optical- infrared spectral energy models for the nuclei of starburst galaxies developed by Siebenmorgen & Krügel (2007) and take Arp 220 as a template for starbursts to calculate the absorption optical depth. For simplicity, we assume all starbursts have the same photon spectra as Arp 220. With such simplifications, the optical depth $\tau_{\gamma\gamma}(E_\gamma)$ in a starburst depends only on its total infrared luminosity L_{TIR} . Fig. 1 shows the corresponding absorption energy E_{cut} (where $\tau_{\gamma\gamma} = 1$) as a function of the total infrared luminosity of starburst galaxies for two choices of $R = 500 \text{ pc}$ and $R = 200 \text{ pc}$. It can be seen that photons with energies above 1 – 10 TeV will be absorbed inside the starburst region.

3.2. Absorbed gamma-rays

The π^0 decay gamma-rays above E_{cut} will be absorbed in the soft photons in the starbursts and produce pairs, each carrying about half energy of the initial photons ($\gamma\gamma \rightarrow e^+e^-$). These pairs, together with the pairs resulted from π^\pm decay, will cool through synchrotron and IC emission. The synchrotron photon energy is $E_{\text{syn}} = 50(E_e/1 \text{ PeV})^2 (B/1 \text{ mG}) \text{ MeV}$, where E_e is the energy of e^\pm pairs and B is the magnetic field in the starburst region. Under reasonable assumptions about the magnetic field in the starburst region, the synchrotron photon energy is below GeV energies, so their contribution to the diffuse gamma-ray flux at $\sim 100 \text{ GeV}$ is negligible. Note that the most constraining point of the gamma-ray background is around 100 GeV, since the observed gamma-ray background flux decreases with the energy. The IC photon energy is $E_\gamma^{\text{IC}} \sim \min[\gamma_e^2 \varepsilon_b, E_e]$, where γ_e is the Lorentz factor of the pair and ε_b is the energy of the soft background photons. Approximating the soft photons as infrared photons with energy $\varepsilon_b = 0.01 \text{ eV}$, The IC photons have energy of $E_\gamma^{\text{IC}} = 5 \text{ TeV} (E_e/10 \text{ TeV})^2 (\varepsilon_b/0.01 \text{ eV})$. The IC photons above E_{cut} will be absorbed and an electro-magnetic cascade will be developed. This cascade process transfers the energy of absorbed gamma-rays to lower and lower energies, until the secondary photons can escape from absorption. The escaped gamma-ray photons can then contribute to the diffuse gamma-ray background. In order to calculate the fraction of the energy loss of e^\pm pairs transferred to the cascade emission, we need to know the energy loss fraction of e^\pm through the IC emission.

3.2.1. Synchrotron vs IC loss

Energy loss timescales are crucial for assessing the fraction of energy loss in these two processes. Thompson et al. (2006) argued that in order for starburst galaxies to fall on the observed FIR-radio correlation, the synchrotron cooling time in starbursts must be shorter than the IC cooling time and the escape time for relativistic electrons. The reason is that, if this constraint is not satisfied, any variation in the ratio between the magnetic field and photon energy density (U_B/U_{ph})

would lead to large changes in the fraction of cosmic ray electron energy radiated via synchrotron radiation. A linear FIR-radio correlation would then require significant fine tuning. The synchrotron timescale depends on the magnetic field in the starburst region. The magnetic fields in starbursts are not well-understood and we parameterize the strength of the magnetic field in terms of the gas surface density Σ_g with the following three scalings :

i) First, in the assumption that the magnetic energy density equilibrates with the total hydrostatic pressure of the interstellar medium, $B \simeq (8\pi^2 G)^{1/2} \Sigma_g$ (Thompson et al. 2006), where G is the gravitational constant. Fields strength as large as this equipartition are possible if the magnetic energy density equilibrates with the turbulent energy density of the ISM. The measurements of Zeeman splitting associated with OH megamasers for eight galaxies suggest that the magnetic energy density in the interstellar medium of starburst galaxies is indeed comparable to their hydrostatic gas pressure (McBride et al. 2014).

ii) $B \propto \Sigma_g^{0.7}$ is sometimes assumed, motivated by setting the magnetic energy density equal to the pressure in the ISM produced by star formation (P_{SF}). Because of $P_{SF} \propto \Sigma_{SFR}$ (where Σ_{SFR} is the star formation rate per unit area) and the Schmidt scaling law for star-formation $\Sigma_{SFR} \propto \Sigma_g^{1.4}$ (Kennicutt 1998), the scaling $B \propto \Sigma_g^{0.7}$ follows.

iii) The third is the minimum energy magnetic field case $B \propto \Sigma_g^{0.4}$, which is obtained using the observed radio flux and assuming comparable cosmic-ray and magnetic energy densities (Thompson et al. 2006). Although such a low magnetic field is not favored, as argued in various aspects (Thompson et al. 2006; McBride et al. 2014), we keep this case in the calculation just to illustrate the difference when a low magnetic field strength is considered.

Thus, the strength of the magnetic fields can be summarized as (Thompson et al. 2006; Lacki & Thompson 2010)

$$\frac{B}{\mu G} = \begin{cases} 2000 \left(\frac{\Sigma_g}{g \text{ cm}^{-2}} \right) & (B \propto \Sigma_g) \\ 400 \left(\frac{\Sigma_g}{g \text{ cm}^{-2}} \right)^{0.7} & (B \propto \Sigma_g^{0.7}) \\ 150 \left(\frac{\Sigma_g}{g \text{ cm}^{-2}} \right)^{0.4} & (B \propto \Sigma_g^{0.4}) \end{cases} \quad (12)$$

As the gas surface density Σ_g scales with the surface density of star formation rate as $\Sigma_g \propto \Sigma_{SFR}^{0.71}$ and the star formation rate ($\pi R^2 \Sigma_{SFR}$) scales linearly with the total infrared luminosity L_{TIR} , we get the relation (assuming a constant star-formation radius R)

$$\frac{\Sigma_g}{g \text{ cm}^{-2}} \simeq 3.6 \left(\frac{L_{TIR}}{10^{12} L_\odot} \right)^{0.71}. \quad (13)$$

The synchrotron energy loss timescale of e^\pm is $t_{syn} = 6\pi m_e c^2 / (c\sigma_T B^2 \gamma_e)$ (Rybicki & Lightman 1979), while the IC energy loss timescale of relativistic e^\pm , for a graybody approximation for the soft background photons, is given by (Schlickeiser & Ruppel 2010)

$$t_{IC} \approx \frac{3m_e c^2}{4c\sigma_T U_{ph}} \frac{\gamma_K^2 + \gamma_e^2}{\gamma_e \gamma_K^2} \quad (14)$$

where $U_{ph} \approx L / (2\pi R^2 c)$ is the energy density of the soft photons, $\gamma_K \approx 4.0 \times 10^7 (T/40K)^{-1}$, T is the temperature of the graybody radiation field and γ_e is the lorentz factor of e^\pm .

Note that Eq.(14) applies to both the Thomson scatterings and the scatterings in the Klein-Nishina regime when γ_e is very high.

The fraction of the energy loss through synchrotron radiation is $t_{syn}^{-1} / (t_{syn}^{-1} + t_{IC}^{-1})$ for one electron or positron of a particular energy. Since this fraction is a function of the energy of e^\pm , we integrate it over a proper energy range to estimate the fraction of the total energy loss of e^\pm through synchrotron radiation in the energy range, which is

$$r \approx \frac{\int_{E_{cut}/2}^{E_{max}/2} \frac{t_{syn}^{-1}}{t_{syn}^{-1} + t_{IC}^{-1}} E_e^{-p+1} dE_e}{\int_{E_{cut}/2}^{E_{max}/2} E_e^{-p+1} dE_e}, \quad (15)$$

where $E_{max} = 4\text{PeV}$ is used for the maximum energy of e^\pm , corresponding to a maximum neutrino energy of 2PeV . We show, in Fig.2, this fraction for starburst galaxies with different L_{TIR} . The black, red and blue lines represent, respectively, the $B \propto \Sigma_g$, $B \propto \Sigma_g^{0.7}$ and $B \propto \Sigma_g^{0.4}$ cases. It shows that for both the $B \propto \Sigma_g$ and $B \propto \Sigma_g^{0.7}$ cases, the synchrotron loss constitute a fraction $\gtrsim 90\%$ of the total energy loss. There are two factors that leads to such a large synchrotron loss fraction: 1) the magnetic energy density is larger than the photon energy density in these cases; 2) the Klein-Nishina effect for e^\pm above $\sim 20(T/40K)^{-1}\text{TeV}$ (Lacki & Thompson 2013) causes the IC energy loss time to increase with γ_e , while the synchrotron loss time continues to fall as γ_e^{-1} .

3.2.2. Cascade gamma-rays

While the synchrotron loss energy goes into low-energy emission and thus does not contribute to the diffuse high-energy gamma-ray background, the IC loss energy will cascade down to the relevant energy range of the diffuse gamma-ray emission. If the cascade develops sufficiently, the spectrum of the cascade emission has a nearly universal form of

$$\Phi_{cas} \propto \begin{cases} E_\gamma^{-1.5} & (E_\gamma < E_{\gamma,b}) \\ E_\gamma^{-2\alpha_\gamma} & (E_{\gamma,b} < E_\gamma < E_{cut}) \end{cases} \quad (16)$$

where E_{cut} is the absorption cutoff energy, $E_{\gamma,b} \approx (4/3)(E_{cut}/2m_e c^2)^2 \varepsilon_b$ is the break energy corresponding to $E_{\gamma,cut}$, and $\alpha_\gamma \simeq 1.8 - 2$ typically (Berezinskii & Smirnov 1975; Coppi & Aharonian 1997). The spectrum above E_{cut} decreases rapidly as $e^{-\tau_\gamma}$. The normalization of the cascade emission spectrum is determined by equating the total cascade energy with the total IC energy loss above E_{cut} , i.e.

$$\int E_\gamma \Phi_{cas} dE_\gamma \simeq \frac{3}{2} (1-r) E_{abs}, \quad (17)$$

where $E_{abs} = \int_{E_{cut}/2}^{E_{max}/2} E_\gamma \Phi_\gamma dE_\gamma$ is the energy of all π^0 -decay gamma-rays above E_{cut} and the factor $\frac{3}{2}$ represents the sum contributions by the π^0 -decay gamma-rays and the gamma-rays from IC scattering of π^\pm -decay e^\pm , the latter of which has a flux about half of that of π^0 -decay gamma-rays.

3.3. Unabsorbed gamma-rays

The gamma-rays from π^0 decay with energies below E_{cut} will escape out of the starburst galaxies and contribute directly to the diffuse gamma-ray background. This flux is model-independent and readily obtained from the observed neutrino flux by using Eq.(10). For a flat neutrino spectrum,

the differential flux of π^0 -decay gamma-rays below E_{cut} is $E_\gamma^2 \Phi_\gamma \simeq 2 \times 10^{-8} \text{GeVcm}^{-2} \text{s}^{-1} \text{sr}^{-1}$.

As we pointed out before, the electrons and positrons accompanying with the neutrino production in the π^\pm decay also contribute to the diffuse gamma-rays through IC scattering of soft background photons. These e^\pm pairs cool by both synchrotron and IC emission. We denote the flux contributed by IC process with $\Phi_{\pi^\pm, IC}$, which is important only when the magnetic energy density in the starburst region is low. Therefore the flux of the unabsorbed gamma-rays is

$$\Phi_{\gamma, un} = (\Phi_\gamma + \Phi_{\pi^\pm, IC}) e^{-\tau_{\gamma\gamma}} \quad (18)$$

Adding the flux of the unabsorbed gamma-rays and that of the cascade gamma-rays, we get the total gamma-ray flux emitted from one starburst galaxy

$$\Phi_{total} = \Phi_{\gamma, un} + \Phi_{cas}. \quad (19)$$

4. THE ACCUMULATIVE DIFFUSE GAMMA-RAY FLUX

Once the gamma-rays escape out of the starburst galaxy, they will further interact with the extragalactic infrared and microwave background photons, and similar cascades are formed for VHE gamma-rays. In this case, however, E_{cut} is different and dependent on the redshift distribution of starburst galaxies. The cascade emission spectrum has the same form as equation (16). Taking such cosmic cascades into consideration, the total gamma-ray flux from one starburst galaxy can be written as

$$\Phi'_{total} = \Phi_{total} e^{-\tau'_{\gamma\gamma}} + \Phi'_{cas}, \quad (20)$$

where $\tau'_{\gamma\gamma}$ is the absorption optical depth due to the extragalactic infrared and microwave background photons and Φ'_{cas} is the flux of the cosmic cascade emission. Then we calculate the accumulative diffuse gamma-ray flux by integrating the contributions of all starburst galaxies in the universe over their redshift and luminosity range, i.e.,

$$E_\gamma^2 \Phi_\gamma^{accu} = \frac{E_\gamma^2 c}{4\pi} \int_0^{z_{max}} \int_{L_{TIR, min}}^{L_{TIR, max}} \frac{\phi(L_{TIR}, z) \Phi'_{total}}{H_0 \sqrt{(1+z)^3 \Omega_M + \Omega_\Lambda}} dL_{TIR} dz. \quad (21)$$

The accumulative diffuse gamma-ray flux are shown in Fig.3 and Fig.4 for the cases of $R = 500\text{pc}$ and $R = 200\text{pc}$ respectively. It can be seen that, the diffuse gamma-ray flux in the case considering the synchrotron loss is less than half of that in the case neglecting the synchrotron loss. This is because that the cascade component resulted from the absorbed gamma-rays is strongly suppressed due to the synchrotron radiation of the e^\pm . The accumulative diffuse gamma-ray flux after considering the synchrotron loss effect contributes $\sim 20\%$ of the observed diffuse gamma-ray background by Fermi/LAT at $\sim 100\text{GeV}$.

For a steeper neutrino spectrum, since the energy fraction in absorbed gamma-rays above E_{cut} is lower, this effect is expected to be less important. As in Murase et al. (2013), we study the allowed range of the spectral index by the observed gamma-ray background data. We find that the index must be $p \lesssim 2.18$, as shown in Fig.5, in order not to violate the observed gamma-ray background data by Fermi/LAT, which is in agreement with the results in Murase et al. (2013).

We also study how much the starburst galaxies in different luminosity ranges and redshift ranges contribute to the diffuse gamma-ray background. Figure.6 shows the contributions in each luminosity range to the total flux. It can be seen that

most flux is contributed by the starbursts in the luminosity range from 10^{11} to $10^{13} L_\odot$. For starburst galaxies of such high luminosity, the pion production efficiency f_π is close to 1 and these galaxies are proton calorimeters. Figure.7 shows the contributions by starburst galaxies in different redshift ranges to the total flux. As expected, the dominant contribution is by starburst galaxies in the redshift range of $1 < z < 2$.

5. DISCUSSIONS AND CONCLUSIONS

Starburst galaxies, which have large amount of supernova or hypernova explosions, are proposed to be a possible source for the sub-PeV/PeV neutrinos recently detected by Ice-Cube (Murase et al. 2013; Liu et al. 2014; Anchordoqui et al. 2014b). We have shown that the minimum diffuse gamma-ray flux associated with these sub-PeV/PeV neutrinos is about $(2-3) \times 10^{-8} \text{GeVcm}^{-2} \text{s}^{-1} \text{sr}^{-1}$, which is a factor of two lower than previous estimates (Murase et al. 2013; Liu et al. 2014). The difference is due to that we here considered the absorption of very high energy photons by the infrared radiation fields inside starbursts and the synchrotron losses of the resulting e^\pm pairs in the strong magnetic fields. This minimum diffuse gamma-ray flux constitute a fraction of $\sim 20\%$ of the observed gamma-ray background flux at $\sim 100 \text{GeV}$ energies, thus leaving a relatively large room for other sources to contribute to the gamma-ray background.

It was proposed that hypernovae remnants in starburst galaxies accelerate protons to $> 10^{17} \text{eV}$ (Wang et al. 2007), which then produce PeV neutrinos via pp collisions with the dense surrounding medium (Liu et al. 2014). Remnants of normal supernovae may accelerate protons to PeV energies, so they may not contribute to the $\gtrsim 100 \text{TeV}$ neutrino flux, but they can produce $< 100 \text{TeV}$ gamma rays, thus contributing to the diffuse gamma-ray background as well. But as long as the diffuse gamma-ray flux contributed by these normal supernovae does not exceed that contributed by the hypernova remnants too much, the total diffuse flux may still fall below the observed background. It may be also possible that, if the remnants of normal supernovae produce a gamma-ray flux 3-4 times higher, the total gamma-ray flux from starburst galaxies can reach the level of the observed one. Interestingly, Tamborra et al. (2014) recently show that star-forming and starburst galaxies can explain the whole diffuse gamma-ray background in the 0.3-30 GeV range.

We thank Ruoyu Liu for useful discussions. This work is supported by the 973 program under grant 2014CB845800, the NSFC under grants 11273016 and 11033002, and the Excellent Youth Foundation of Jiangsu Province (BK2012011).

REFERENCES

- Aartsen, M. G., Ackermann, M., Adams, J., et al. 2014, arXiv:1405.5303
- Abdo, A. A., et al. 2010, Phys. Rev. Lett., 104, 101101
- Ahlers, M., & Murase, K. 2013, arXiv:1309.4077
- Anchordoqui, L. A., Hooper, D., Sarkar, S., & Taylor, A. M. 2008, Astroparticle Physics, 29, 1
- Anchordoqui, L. A.; Goldberg, H.; Lynch, M. H. et al. 2014a, Phys. Rev. D, 89, 083003
- Anchordoqui, L. A., Paul, T. C., da Silva, L. H. M., Torres, D. F., & Vlcek, B. J. 2014b, arXiv:1405.7648
- Berezinsky, V., Gazizov, A., Kachelrieß, M., & Ostapchenko, S. 2011, Physics Letters B, 695, 13
- Berezinskii, V. S., & Smirnov, A. I. 1975, Ap&SS, 32, 461
- Bonometto, S., & Rees, M. J. 1971, MNRAS, 152, 21
- Coppi, P. S., & Aharonian, F. A. 1997, ApJ, 487, L9

- Fox, D. B.; Kashiyama, K.; Mészáros, P., 2013, *ApJ*, 744, 74
- Grupponi, C., Pozzi, F., Rodighiero, G., et al. 2013, *MNRAS*, 432, 23
- He, H.-N.; Liu, R. Y.; Wang, X. Y.; Nagataki, S.; Murase, K.; Dai, Z. G., 2012, *ApJ*, 752, 29
- He, H.-N.; Wang, T.; Fan, Y.-Z.; Liu, S.-M.; Wei, D.-M., *Phys. Rev. D*, 87, 063011
- Kalashov, O. E., Semikoz, D. V., & Sigl, G. 2009, *Phys. Rev. D*, 79, 063005
- Kalashov, O. E., Kusenko, A. and Essey, W., 2013, *Phys. Rev. Lett.*, 111, 041103
- Kennicutt, R. C., Jr. 1998, *ApJ*, 498, 541
- Lacki, B. C., & Thompson, T. A. 2010, *ApJ*, 717, 196
- Lacki, B. C., & Thompson, T. A. 2013, *ApJ*, 762, 29
- Lacki, B. C., Thompson, T. A., Quataert, E., Loeb, A., & Waxman, E. 2011, *ApJ*, 734, 107
- Liu, R.-Y., Wang, X.-Y., 2012, *ApJ*, 746, 40
- Liu, R.-Y., Wang, X.-Y., 2013, *ApJ*, 766, 73
- Liu, R.-Y., Wang, X.-Y., Inoue, S., Crocker, R., & Aharonian, F. 2014, *Phys. Rev. D*, 89, 083004
- Loeb, A., & Waxman, E. 2006, *JCAP*, 5, 3
- Lunardini, C., Razzaque, S., Theodoseou, K. T., & Yang, L. 2013, arXiv:1311.7188
- McBride, J., Quataert, E., Heiles, C., & Bauermeister, A. 2014, *ApJ*, 780, 182
- Murase, K., Ahlers, M., & Lacki, B. C. 2013, *Phys. Rev. D*, 88, 121301
- Murase, K., & Ioka, K. 2013, *Physical Review Letters*, 111, 121102
- Neronov, A., Semikoz, D., & Tchernin, C. 2014, *Phys. Rev. D*, 89, 103002
- Razzaque, s., 2013, *Phys. Rev. D*, 88, 081302
- Rybicki, G. B., & Lightman, A. P. 1979, New York, Wiley-Interscience, 1979. 393 p.,
- Schlickeiser, R., Elyiv, A., Ibscher, D., & Miniati, F. 2012, *ApJ*, 758, 101
- Schlickeiser, R., & Ruppel, J. 2010, *New Journal of Physics*, 12, 033044
- Siebenmorgen, R., & Krügel, E. 2007, *A&A*, 461, 445
- Stecker, F. W., Done, C., Salamon, M. H., & Sommers, P. 1991, *Physical Review Letters*, 66, 2697
- Stecker, F. W., & Salamon, M. H. 1996, *ApJ*, 464, 600
- Stecker, F. W., 2013, *Phys. Rev. D* 88, 047301
- Tacconi, L. J., Neri, R., Chapman, S. C., et al. 2006, *ApJ*, 640, 228
- Tamborra, I., Ando, S. & Murase, K. 2014, arXiv:1404.1189
- Taylor, A. M., Gabici, S., & Aharonian, F. 2014, *Phys. Rev. D*, 89, 103003
- Thompson, T. A., Quataert, E., Waxman, E., Murray, N., & Martin, C. L. 2006, *ApJ*, 645, 186
- Trotta, R., Jóhannesson, G., Moskalenko, I. V., et al. 2011, *ApJ*, 729, 106
- Wang, X.-Y., Razzaque, S., Mészáros, P., & Dai, Z.-G. 2007, *Phys. Rev. D*, 76, 083009
- Wang, X. Y., Liu, R. Y. & Aharonian, F., 2011, *ApJ*, 736, 112
- Waxman, E., & Bahcall, J. 1997, *Physical Review Letters*, 78, 2292
- Winter, W., 2013, *Phys. Rev. D*, 88, 083007

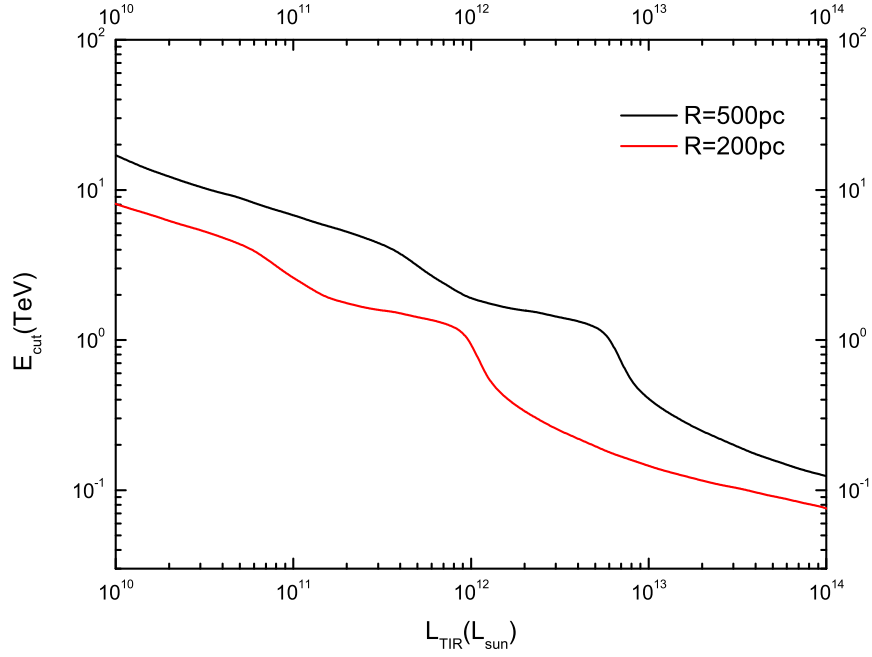


Figure 1. The absorption cutoff energy of VHE gamma-rays by soft photons in starburst galaxies with different L_{TIR} .

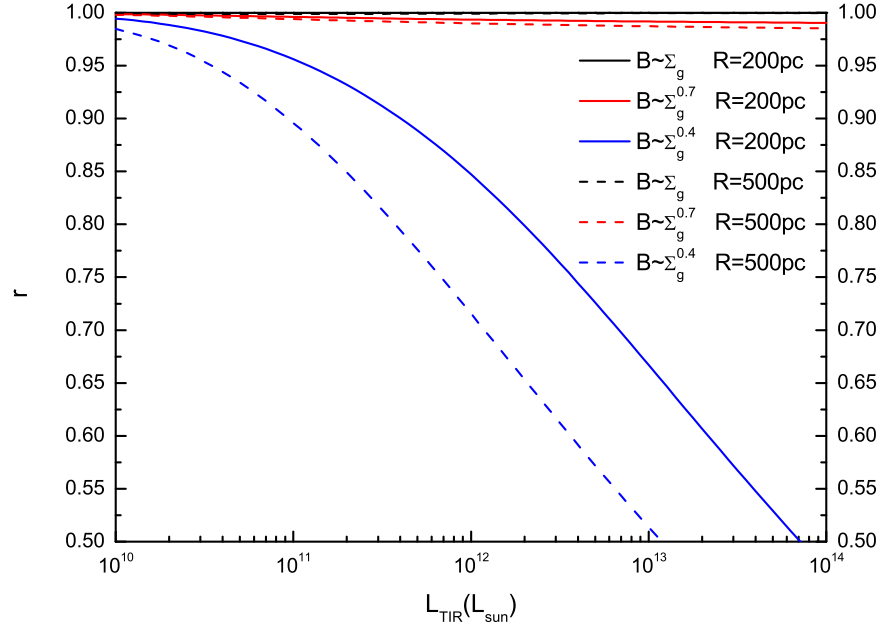


Figure 2. The fraction of total energy loss of relativistic e^{\pm} through the synchrotron radiation in the starburst magnetic field. The solid and dashed lines represent the cases of $R = 200\text{pc}$ and $R = 500\text{pc}$, respectively. The black, red and blue lines show the cases of $B \propto \Sigma_g$, $B \propto \Sigma_g^{0.7}$ and $B \propto \Sigma_g^{0.4}$, respectively. Note that the $B \propto \Sigma_g$ lines overlap with the frame of the figure.

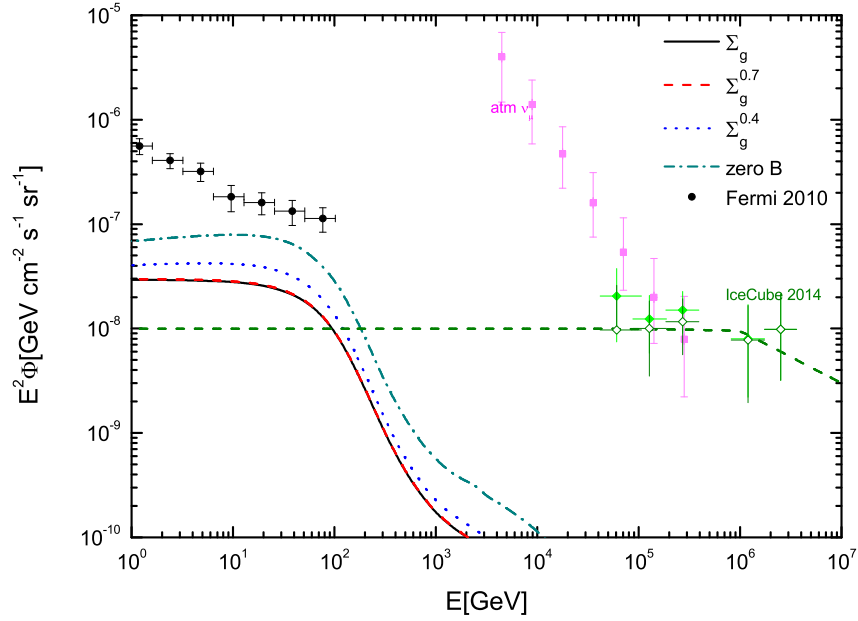


Figure 3. The accumulative diffuse gamma-ray flux of starburst galaxies for different assumptions of the magnetic fields in the starburst region. $R = 500\text{pc}$ and $p = 2$ are assumed. The black, red and blue lines show the cases of $B \propto \Sigma_g$, $B \propto \Sigma_g^{0.7}$ and $B \propto \Sigma_g^{0.4}$, respectively. For illustration, the green line shows the case of $B = 0$. The neutrino flux is obtained using Eq.(7). The extragalactic gamma-ray background data from Fermi/LAT are depicted as the black dots. The atmospheric neutrino data and the IceCube data are also shown.

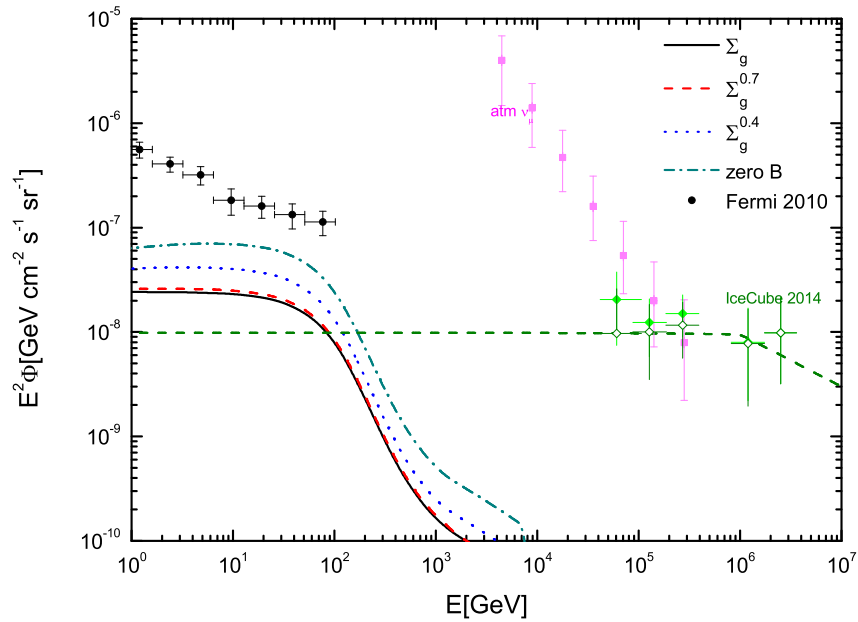


Figure 4. The same as figure 2, but with $R = 200\text{pc}$.

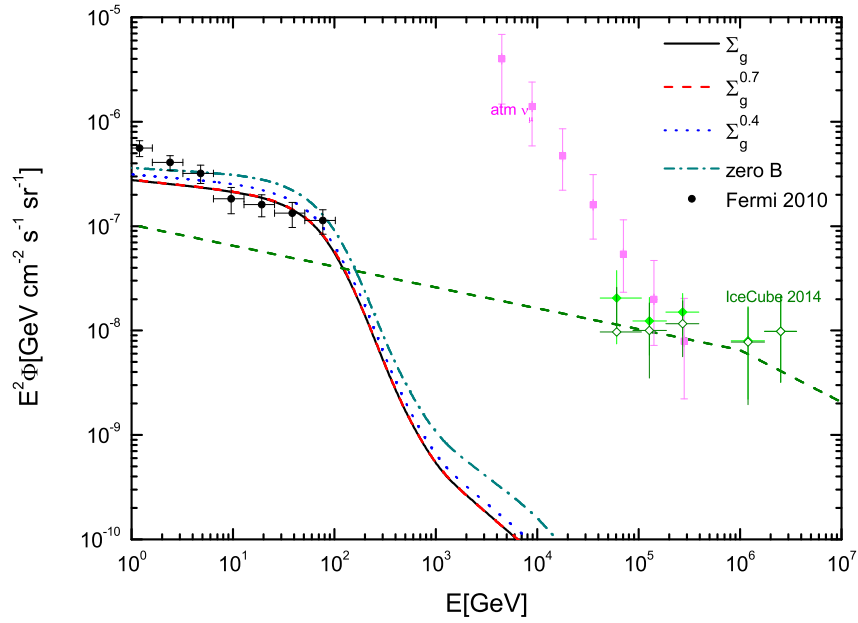


Figure 5. The same as figure 2, but assuming a steeper proton spectrum with $p = 2.18$

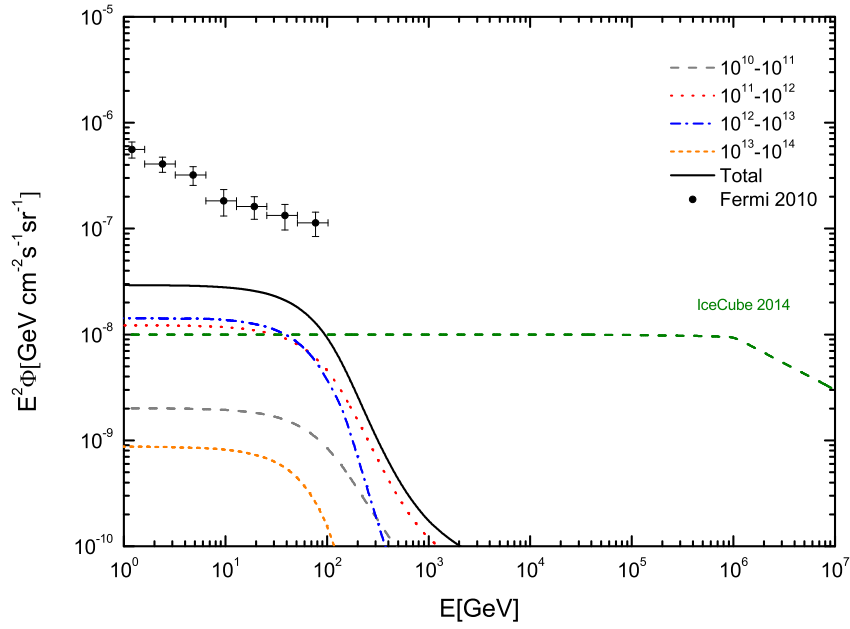


Figure 6. The diffuse gamma-ray flux contributed by starburst galaxies in different luminosity ranges. The grey, red, blue and orange lines represent the contributions by the starburst galaxies in the luminosity ranges of $10^{10} - 10^{11} L_{\odot}$, $10^{11} - 10^{12} L_{\odot}$, $10^{12} - 10^{13} L_{\odot}$, and $10^{13} - 10^{14} L_{\odot}$, respectively. The black line represents the sum of them. $R = 500\text{pc}$, $B \propto \Sigma_g$ and $p = 2$ are assumed.

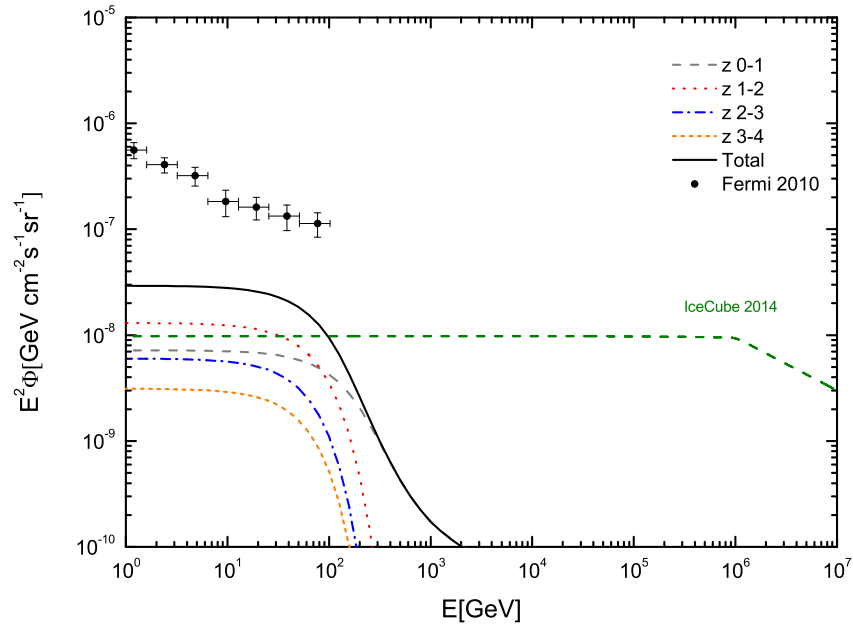


Figure 7. The diffuse gamma-ray flux contributed by starburst galaxies in different redshift ranges. The black, red, blue, green, and purple lines represent the contributions by the starburst galaxies in the redshift ranges of 0–1, 1–2, 2–3 and 3–4, respectively. The black line represents the sum of them. $R = 500\text{pc}$, $B \propto \Sigma_g$ and $p = 2$ are assumed.